MET.O.14

METEOROLOGICAL OFFICE
BOUNDARY LAYER RESEARCH BRANCH
TURBULENCE & DIFFUSION NOTE

T.D.N. No. 94

Micrometeorological Characteristics of the 1976 Hot Spells

by

C.J.Richards

August 1978

Micrometeorological Characteristics of the 1976 Hot Spells.

By C J Richards.

Summary

The memorable weather at Cardington during the period June to August 1976 is described from the micrometeorological viewpoint of the energy budget over a grass-covered surface. The flux of sensible heat from the surface to the overlying air was a dominant term in the energy budget for much of this period, and reached the exceptionally high value of 300 Wm^{-2} on some days in August. However, during the hottest period at the end of June, latent heat of evaporation also constituted a significant component of the energy budget. Measurements are presented to illustrate the noteworthy diurnal variation of soil heat flux (reaching 100 Wm^{-2}), and of surface layer temperature during fine weather this summer.

1. Introduction

Much attention has been paid recently to the severe drought of 1975-76 over the British Isles. Perry (1976) has described the twelve-month period starting on 1 May 1975 as the driest period over the United Kingdom since records began, with only 60 percent of normal rainfall in parts of the Midlands and Southwest England. The period from 23 June to 8 July 1976, in particular, was exceptionally hot and dry; see Shaw (1977). At Cardington, Beds, the maximum temperature exceeded 30°C every day throughout this period. The hydrological and dynamical aspects of this drought have been described by Murray (1977), Green (1977), Ratcliffe (1977), and Miles (1977). However, one important aspect has not yet been discussed in detail, ie the micrometeorology of the surface boundary layer during this period, and particularly the heat budget at the surface. The surface layer, which comprises the lowest few tens of metres of the atmosphere, is a very important region for many reasons. Man's activities are largely confined to it and, of course, many of the basic energy transformations occur within it.

On a cloudless day, incoming solar radiation absorbed at the earth's surface is converted into heat, and the nature of this energy conversion very much depends upon the character of the underlying surface. For a typically rural land surface the incoming radiant energy is converted (a) into latent heat of evaporation, and (b) ordinary (or "sensible") heat. Some of this sensible heat is conducted down into the ground, and the rest is used to warm the overlying air through a combination of eddy diffusion, radiative, and molecular conduction processes; see, for example Munn (1966).

At the Meteorological Research Unit at Cardington an experiment is presently being carried out to assess the nature of the energy budget over a grass-covered surface, and to study its behaviour on a variety of timescales. Some measurements were made during the summer of 1976 and they indicate that conditions quite unusual to rural England developed in the surface layer at this time. Before the energy budget is discussed, however, the terms in the balance equation will be defined and the method used to measure them briefly outlined.

2. Definition of the Surface Energy Balance Equation

From the principle of conservation of energy it is clear that all gains and losses of energy at the earth's surface must balance. For a uniform, horizontal land surface this balance can be described by the equation:

$$R_N = H + G + LE \quad \ldots\ldots (1)$$

where R_N is the net receipt of radiant energy, H is the flux of sensible heat transferred from the surface to the overlying air, G is the downward flux of heat into the soil, and LE is the energy required to evaporate surface moisture. R_N represents a radiation balance among the following components: (refer to Fig 1)

Q_1 = direct, shortwave radiation - the solar beam;
Q_2 = diffuse, shortwave radiation - scattered from clouds and the atmosphere;
Q_3 = shortwave radiation scattered by the surface - upwards;
Q_4 = longwave emission from the atmosphere - downward; and
Q_5 = longwave emission from the ground - upward.

Therefore $R_N = Q_1 + Q_2 + Q_4 - Q_3 - Q_5$ .... (2)

Positive R_N represents a net gain (or warming), and $R_N < 0$ a net loss (or cooling) of radiant energy.

Positive H is associated with an unstable temperature stratification in the surface boundary layer, that is when the (dry bulb) potential temperature falls with height; whereas negative $H < 0$ occurs with a stable layer $(\frac{d\theta}{dz} > 0)$.

The downward soil heat flux G is positive when the temperature of the soil near the surface decreases with depth.

The latent heat flux LE equals the rate of evaporation E, multiplied by the latent heat of vapourisation L_v thus:

$$LE = L_v \times E \quad \ldots\ldots\ldots \quad (3)$$

R_E

and is positive when the surface is losing moisture to the air. LE may be negative, for example when dew is forming.

The components of the energy balance equation are defined in terms of their flux intensities, and their units are watts per sq metre ($W m^{-2}$). In these units the solar constant $S = 2{\cdot}0\,\text{cals.cm}^{-2}\,\text{min}^{-1} = 1400\ W m^{-2}$.

For a vegetated surface LE in equation (1) represents the sum of the energy loss due to evaporation of moisture in the surface layer of the soil, together with the transpiration of vapour from the vegetation cover itself, and is termed "evapotranspiration". "Potential evapotranspiration" is the evaporation which occurs if soil moisture is not a limiting factor, but in practice the actual evaporation depends very much on the available water in the ground. Since Transpiration is the transfer of water from soil to the atmosphere via a plant, & it tends to short circuit the normal channels of vertical soil moisture transfer, such as capillary action. Water loss through evaporation therefore tends to be faster from a plant-covered soil than from a bare surface, and the available soil moisture supply is likely to be depleted sooner unless replenished by rainfall.

3. Measurement of the Energy Balance

The experimental site at Cardington lies about 4 km southeast of Bedford, within a broad clay vale which provides an excellent exposure in many directions.

Both the site and its immediate surroundings are grass-covered, but the surface of the agricultural land beyond is more varied, ranging from arable and cereal crops to rough pasture and small woods. The fetch over grass is limited to between 400 and 800 m, and this restricts the constant flux layer at the site to a depth of little more than 4 m.

Net radiation R_N in equation (1) is measured directly with a ventilated radiation balance meter at a height of around 1 m, and measurements are accurate to between 5 and 10 percent. Soil heat flux G is an extrapolated estimate of the surface value based on measurements at several levels below the surface; see eg. Blackwell (1963). Five suitably calibrated flux plates were installed in the soil at depths of 5, 10, 20, 40 and 80 cm. The top flux plate lay in contact with the root system of the thick turf which forms the surface. The estimate of G is based on extrapolation of measurements at 5, 10 and 20 cm and confidence in this quantity is limited to around 20 percent. Latent heat flux (LE) is derived from hourly measurements of the evapotranspiration from the short-cropped grass surface of a weighing lysimeter, (Blackwell, 1963). The lysimeter is a square tank of surface area 2 m^2 and depth 50 cm, and it contains a sample of soil representative of the surrounding site. The change in the mass of this tank due to evaporation from the grass surface or rainfall upon it is monitored automatically, and LE is derived from equation (3). This device has proved to be a direct and quite reliable means of measuring LE, with an accuracy of between 10 and 20 per cent. However, it cannot normally be used to measure LE over a period of less than one hour. In addition to evaporation from grass, daily measurements are also made of the evaporation from an exposed water surface, using a Met Office British standard evaporation tank.

The sensible heat flux H cannot be measured as readily as can R_N, G, or LE. Two indirect methods have been used to estimate H : (a) from the gradient of potential temperature, through the transport equation

$$H = -\rho C_p K_h \, d\theta/dz \quad \ldots\ldots\ldots\ldots \quad (4);$$

and (b), through the residual technique, in which H is expressed explicitly in terms of R_N, G and LE, thus

$$H = R_N - G - LE \quad \ldots\ldots\ldots \quad (5)$$

In the first method K_h is the eddy diffusivity for heat transfer. It is not a physical constant but depends on various turbulence characteristics such as wind shear, stability, and height above the surface. Its height variation in the surface layer is described by a semi-empirical relationship of the form

$K_h = \frac{k u_* z}{\phi_h}$; see, for instance, Sutton (1953), or Priestley (1959). The nondimensional function ϕ_h can be calculated from the Richardson number; see, for example, Businger et al (1971), and this in turn is derived from the vertical profiles of wind speed and potential temperature, averaged over a suitable period such as 20 minutes. Measurements of wind speed and temperature are made at Cardington at heights of 0.5, 1,2,4,8 and 16 m using lightweight photo-electric cup anemometers and standard platinum-in-steel resistance thermometers, the latter being suitably screened from direct-radiation. These measurements enable both u_* and ϕ_h, and therefore K_h and H to be calculated.

The accuracy with which the sensible heat flux can be calculated from equation (4) is limited by the semi-empirical description of the eddy diffusivity K_h.

At Cardington, it is also limited by the restricted fetch over a uniform grass surface, and consequently by the relatively shallow constant flux layer at the site. For these reasons the sensible heat flux cannot normally be measured by this method to an accuracy of better than 20 percent. The validity of the residual estimate of using equation (5) depends, of course, upon the energy balance equation (1) being obeyed in the first place. Measurements of R_N, G, LE and H, in widely varying conditions at different times of the year, do indeed show that this balance equation is satisfied, within the error limits mentioned above.

4. The Surface Energy Budget at Cardington: June - August 1976

Fig 2 highlights the exceptionally dry character of the weather during this summer. This diagram shows the monthly rainfall and evaporation from March to October 1976 at Cardington. The evaporation from an open water surface and the evapotranspiration from grass are both compared with the average for the previous six years. It is noteworthy that evaporation from water reached a maximum of 156 mm during July, 160 percent of the average, and this figure would probably be typical of the water loss from rivers, lakes and reservoirs. On the other hand, evapotranspiration fell steadily from late spring to the very low values of less than 30 mm during July and August, approximately 40 percent of the average.

Shown in Fig 3 is the daily variation of the components in the energy budget at Cardington from the middle of June to the end of August 1976. The data presented are averages over the period 0600 to 1800 GMT: Daily rainfall is included in the diagram, and it will be noted that greater than 1 mm of rain fell on only seven days during this period. The daily maximum temperature is also shown and two hot spells, labelled "1" and "2", respectively, have been defined. The first of these, Hot Spell 1, covers the period from the 23 June to 8 July, when the maximum temperature exceeded 30°C daily. The second, Hot Spell 2, represents a fortnight in the middle of August, the 11-26th, when the temperature generally exceeded 26°C.

It will be noted from Fig 3 that, of the four components in the energy budget, the radiation R_N is typically the largest. The net radiation shows a steady decrease during the summer, falling erratically from a peak during Hot Spell 1 to a minimum in early August, but increasing again slightly during Hot Spell 2. Individual components can change rapidly in magnitude from one day to the next; see, for instance, the two periods 15-22 June and the 15-18 July. The net radiation is usually subject to the greatest change because it is strongly dependent on external factors such as cloud cover and depth, and on turbidity (or pollution). The other components of the budget reflect changes in R_N to a varying degree. The soil heat flux, for instance, falls during the same period as R_N, between Hot Spell 1 and the beginning of August.

A detailed analysis of the hourly energy balance for the four days labelled A to D in Fig 3 is presented in Figs 4(a)-4(d), and they illustrate aspects of the diurnal surface energy budget during the summer of 1976. On fine days the mean hourly net radiation reaches a maximum of between 400 and 500 Wm^{-2}; see Figs 4(b)-4(d). The shape of the R_N curve on a clear day is not perfectly sinusoidal, unlike the incident-shortwave component Q_1 (refer to Fig 1). Soil heat flux G tends to lag in phase behind the net radiation by an hour or so, as is illustrated in Figs 4(a), 4(c). This phase lag, to be described in some detail in section 6, implies that G is not a true "surface" value, and it probably reflects a limitation of the extrapolation method discussed earlier. It also throws doubt on the validity of equation (5) for estimating H when G is changing rapidly.

During the summer both the latent heat and sensible heat fluxes behave very differently from R_N and G. Well before the arrival of Hot Spell 1 the latent heat flux was a significant term in the energy budget, following rain in the middle of June, and this is exemplified on the 20 June, shown in Fig 4(a). Apart from the radiation term, LE dominates the energy budget for much of this day. During the morning of the 20 June the latent heat flux increases so rapidly in response to the radiation that it drives the sensible heat flux strongly negative for an hour or so until 1000 GMT. Shortly after midday, however, the rate of evaporation decreases, and allows the sensible heat flux to build up well into the afternoon. It is worth noting the effect which the large latent heat and relatively small sensible heat fluxes have had on the air temperature. After a gradual increase during the day, a maximum of only 20°C is reached, and this occurs as late as 1600 GMT.

During Hot Spell 1 the latent heat flux falls rapidly to a low level, and the sensible heat component becomes more important. By the 30 June (Fig 4c) LE falls to between 10 and 15 per cent of the net radiation during the midday hours, in marked contrast to the situation at the beginning of the hot spell. During July and August LE remains very small, and H dominates the surface energy budget. This pattern is, however, temporarily interupted in the middle of July after a rainfall of over 20 mm on the 16th. The modest recovery of the latent heat flux in the energy budget afterwards is shown in Fig 3. In the absence of further rainfall, LE decreases again during the period leading up to Hot Spell 2. A large reservoir of soil moisture is necessary to support evapotranspiration from a plant cover at the potential rate, particularly during the summer when the relative humidity is low; see Penman (1949). This effect is illustrated in Fig 5, which compares the daily evaporation from water with that from grass during Hot Spell 1. It is worth contrasting the slow, but sustained decline in evapotranspiration from grass, from 2 mm. day^{-1} to less than 0.5 mm. day^{-1}, with the evaporation from water during the period. The latter reaches a maximum of 9 mm on

30 June, coinciding with a minimum relative humidity of 11 per cent that afternoon.

Throughout Hot Spell 2 the sensible heat flux H remains a conspicuously dominant term, alone accounting for around 70 percent of the available radiant energy. Evaporation from the ground reached its lowest value of the season at this time, with a daytime latent heat flux of only 30-40 W m^{-2}. The detailed budget for 16 August (Fig 4d) reflects the diurnal variation of its components toward the end of the summer, and it shows characteristics similar to those measured during the latter half of Hot Spell 1; compare Figs 4(c) and 4(d). G and LE are smaller on the 16 August but the sensible heat flux H reaches the remarkably high value of 300 Wm^{-2} during the middle of the day.

As evaporation falls during Hot Spell 1, the hourly dependence of LE on R_N which is very strong on the 20 and 26 June (Figs

4(a), 4(b), also weakens. By July, in fact, the latent heat flux is virtually independent of the incident radiation, and it responds to secondary influences when these become available - eg surface moisture. This effect is especially noticeable around dawn, following overnight dew or fog deposition, and is then almost as large as it is around midday see, for instance, Figs 4(c), 4(d). On several days during Hot Spell 2 the latent heat flux was a maximum shortly after dawn. At Cardington the ground was baked hard and cracked during July and August, yet the lysimeter was still recording some water loss through transpiration, although it amounted only to 0.4 mm day^{-1}. Evaporation measurements from non-irrigated lysimeters are often criticised for being unrealistically small during periods of drought. However, during the summer of 1976 the grass cover on the lysimeter remained representative of its surroundings.

5(a). Relation between Atmospheric Structure, Surface Energy Budget, and Maximum Temperature.

Although the magnitude of the sensible heat flux H expresses the amount of energy available for warming the lower layers of the atmosphere, the daily changes in H are not, ofcourse, necessarily correlated with those of surface temperature. On some days this correlation is more closely marked, as for instance on the 18, 19 June and the 16, 18 July; see Fig 3. On the other hand, during the period 26-30 June H increased by about 50 percent, yet the highest temperature at Cardington during Hot Spell 1 was recorded on the 26 June, when the sensible heat was not much larger than the latent heat flux. The explanation for this is apparent from inspection of Fig 6, which shows the temperature structure of the lowest kilometre or so of the atmosphere at 0600 GMT on the 26, 30 June, and

16 August, derived from the Cardington BALTHUM ascents. On the 26 June a layer of potentially very warm air was based at the surface, but by the 30th advection from the North Sea had cooled this layer considerably. This had the effect of generally increasing the depth of the convective boundary layer, and consequently restricting the rise in surface temperature on the 30th. The amount of heating on these two days has been calculated from the sensible heat flux curves shown in Figs 4(b), 4(c), neglecting other influences such as advection, radiation, entrainment, etc. The arrowed adiabats AB and CD in Fig 6 represent the estimated maximum potential temperature of the convective layer on the 26th and 30th, respectively. If an extra 2°C is allowed for the superadiabatic near the surface, these adiabats imply afternoon screen temperatures of around 31.5° and 28°C, which compare well

with the actual values of 34° and 30°C, respectively.

Also shown in Fig 6 is the temperature structure on the 16 August, when the surface energy budget was dominated by a large sensible heat flux. The adiabat EF represents the estimated maximum boundary layer depth on this day. An afternoon screen temperature of around 25° is predicted, and this compares with an actual temperature of between 26° and 27°C.

5(b) Diurnal Variation of Surface Layer Temperature

Since the sensible heat flux H and the vertical temperature gradient are related through equation (4), a day has been chosen from Hot Spell 2 to illustrate how the surface layer temperature changed on one particular fine day during the summer of 1976. Fig 7 shows isotherms on a log height (z)-time plot, and the following points may be noted.

(i) The overnight nocturnal inversion

in the surface layer reaches its maximum strength between 0400 and 0500 GMT, ie an hour or so before dawn.

(ii) The inversion breaks down from the surface, and a near neutral layer establishes itself for approximately an hour, during which period air temperature increases quickly.

(iii) During the morning the static instability of the layer increases steadily. A superadiabatic temperature gradient develops, with a temperature lapse of between 2° and $2.5^{\circ}C$ being produced through the 0.5 m to 16 m layer. This was fairly typical of the lapse rate on a fine summer day in 1976.

(iv) In the late afternoon the layer begins to cool, and it passes through the transitional phase of neutrality at around 1800 GMT ie one hour before sunset. During the evening an inversion develops, and this slowly strengthens, accompanied by a steady cooling at all levels. This cooling is considerably less rapid than the warming which occurs immediately after dawn.

6. Diurnal Variation of Soil Heat Flux

Before discussing the characteristics of soil heat flux at various depths, it is necessary to review briefly the relationships governing heat flow in the ground. All natural ground consists essentially of (a) soil, (b) free water, and (c) air pockets between the soil particles. The relative proportion of these components governs the density ρ and specific heat C of the soil at any depth z. The specific heat per unit volume (ρC) is constant for dry soil, but increases with the water content of the soil; for example, see Geiger (1950). The rate of flow of heat through soil G is given by the classical conductivity equation

$$G = -k_s \, dT/dz \quad \ldots\ldots\ldots \quad (6)$$

where k_s is the thermal conductivity and dT/dz is the temperature gradient in the soil. Conductivity varies with density and soil water content, being considerably greater in wet soil than in dry.

The rate of change of soil temperature can be related to the divergence of soil heat flux G through the equation:

$$dT/dt = -1/(\rho C) \frac{dG}{dz} \quad \ldots\ldots\ldots \quad (7)$$

Eliminating G from (6) and (7), and assuming k_s is constant with depth, leads to the heat conduction equation in one dimension:

$$dT/dt = K \, d^2T/dz^2 \quad \ldots\ldots\ldots \quad (8)$$

$$\text{where} \quad K = k_s/\rho C \quad \ldots\ldots \quad (9),$$

is the thermal diffusivity of the soil (units: $m^2\ sec^{-1}$). If a sinusoidal time-dependent boundary condition, with angular frequency ω is applied at the surface ($z=0$), in order to simulate the daily radiation wave at the surface, a solution can be derived for the soil heat flux G in the form:

$$G(z,t) = G_0 \exp\left[-z\sqrt{\frac{\omega}{2K}}\right] \sin\left(\omega t - z\sqrt{\frac{\omega}{2K}}\right) \quad \ldots\ldots(10)$$

if K is constant with z.

This describes a progressive wave of phase velocity V, given by

$$V = \sqrt{2K\omega} \quad \ldots\ldots\ldots \quad (11)$$

whose amplitude decays exponentially and lags in phase with depth. G_0 is the surface amplitude. The amplitude, A_z, of the soil heat wave at any depth z is related to the amplitude, A_{ref}, at some given depth Z_{ref} through the equation:

$$A_z / A_{ref} = \exp\left[\sqrt{\frac{\omega}{2K}}\left(Z_{ref} - Z\right)\right] \quad \ldots\ldots(12)$$

This equation can be used to determine the "penetration depth" of either the daily or annual heat wave into various soils.

This depth is defined as the level at which the amplitude of the soil heat wave is reduced to one percent of its surface value.

Hot Spell 1 produced some notable diurnal variations in soil heat flux, with fluxes near the surface regularly exceeding 100 Wm^{-2} by day. Fig 8 shows the profiles of soil heat flux on 26 June at depths of 5, 10, 20, 40 and 80 cm, with the surface net radiation R_N included for comparison. Note the increasing time (phase) lag of the profile maxima as the heat wave is conducted down through the soil; this is predicted by equation (10). It takes about 11 hours for the wave to reach a depth of 40 cm, giving a mean phase velocity of around 3.5 cm hr^{-1}. The angular frequency ω is obtained from the half period of the wave motion, which is 10 hours. Since ω and V are known, equation (11) gives a value of $K = 0{\cdot}54 \times 10^{-6} \, m^2 \, sec^{-1}$

for the mean diffusivity in the top 40 cm layer of soil. The penetration depth of the diurnal soil heat wave can now be calculated from equation (12). This value, 51 cm, fits the experimental data in Fig 8 well, since at 40 cm depth the wave amplitude is very small, and at 80 cm the diurnal influence has disappeared. The steady downward flux of 5 Wm^{-2} at this lowest level reflects longer term changes in soil temperature. Equation (12) may also be used to compare the observed amplitude reduction with depth on the 26 June with the theoretical ratio A_z/A_{ref} . This reduction ratio is shown in column 2 of Table 1, expressed in terms of the 5 cm amplitude, A_5 . Column 3 in this table gives the observed soil heat flux amplitude. By multiplying the percentages in column 2 with the observed 5 cm amplitude, the theoretical amplitude variation with depth is obtained, as shown in column 4. A comparison of columns 3 and 4 suggests that the observed amplitude decay agrees well with the exponential law of equation (12). The agreement is not perfect because soil is not a homogeneous medium. Both the conductivity and density can vary considerably with depth, due to changes in the composition of the soil; and this implies that the diffusivity K and phase velocity V are not constant. In order to illustrate this point, Fig 8 shows that the speed of the soil heat wave through the 10-20 cm layer is twice that through the 20-40 cm layer. It should, however, be noted that K is rather insensitive to changes in soil moisture since it is the ratio of two parameters (refer to equation 9), both of which vary in the same sense with changes in soil water content.

In Fig 9 isopleths of soil heat flux are shown on a depth-time plot over a three day period during Hot Spell 1. The gradient of the two sloping lines on this diagram gives the mean downward velocity of the heat wave into the ground. The diagram highlights the remarkable changes in heat flux which occurred within the top 20 cm layer of soil during fine weather in the summer of 1976. It also demonstrates how difficult it can be to obtain a realistic measure of the surface heat flux in these circumstances. It is worthwhile comparing the magnitude of the soil heat flux in this layer with that measured during a more recent hot spell at the beginning of July 1977, when the ground water content was very high. Normalized in terms of the net radiation, the amplitude of the soil heat flux in the top 20 cm layer was between 50 and 100 percent greater during Hot Spell 1 than in July 1977. However, equations (6) and (7) show that, in the presence of a given heat flux G, the rate of change of temperature and the vertical temperature gradient in the ground are inversely proportional to the specific heat,

(ρC) and conductivity, k_s . Since (ρC) and k_s both decrease with soil moisture content, it is likely that the amplitude of the diurnal temperature change in this top layer of soil during Hot Spell 1 became even more pronounced than that of the soil heat flux.

7. Concluding Remarks

For much of July and August 1976 between 75 and 90 percent of the available incoming radiation was used to heat the ground and the air above, with the rest passing into latent heat of evaporation. During Hot Spell 2 in the middle of August the sensible heat flux regularly reached 250 - 300 Wm^{-2}, by day, with the latent heat flux accounting for less than 40 Wm^{-2}. At the start of the June-July hot-spell, however, over 30 percent of the available energy was being used for evaporation, with the latent heat flux then exceeding 100 Wm^{-2} during the day. The amplitude of the surface soil heat flux reached notably high values of over 100 Wm^{-2}

at this time. In order to emphasize the exceptional nature of the energy budget during the summer of 1976, it is worthwhile considering the change in the Bowen ratio, H/LE. In an average summer with a regular rainfall, this ratio varies between 0.5 and 1.0 during the day, that is, the latent heat flux often exceeds the sensible heat component. During 1976, however, the Bowen ratio increased to well over 6 during August.

Ratcliffe (1976) has estimated that during June 1976 approximately 70 percent of the total net incoming radiation was available for heating the ground and air over the country as a whole. This is in excellent agreement with the value of 68 percent measured on the 26 June at Cardington when the highest temperature of the season was recorded. However, sensible heating is clearly not the only factor controlling surface temperature; atmospheric temperature structure is just as important. This point is demonstrated by the variation of the ratio $(H+G)/R_N$ during the summer, which reached a maximum during the hot spell in the middle of August. For example, on the 16 August the normalized combined sensible and soil heat flux was 25 per cent greater than on the 26 June, yet the maximum temperature on the August day was 7°C lower. This would suggest that, at Cardington, the depth of the convective boundary layer exerted a more important influence than sensible heating in producing the particularly high screen temperature maxima in the last week in June.

Acknowledgements

Thanks are due to my colleagues at the Meteorological Research Unit for their assistance during this experiment, and especially to the technical staff for their invaluable support, both in the field and in the recording laboratory.

References

Blackwell, M J	1963	"The role of evaporation in the surface energy balance". The Water Relations of Plants. Blackwell Scientific Publications.
Businger, J A., S C Wyngaard, Y Izumi, and E F Bradley	1971	"Flux Profile Relationships in the Atmospheric Surface Layer" J.Atmos. Sci 28 p 181-189
Geiger, R	1950	"The Climate near the ground" Harvard University Press, Cambridge, Mass (revised edition 1965)
Green, J S A	1977	"The Weather during July 1976 - some dynamical considerations of the drought" WEATHER 32 No 4, p 120-126
Miles, M K	1977	"Atmospheric circulation during the severe drought of 1975/76" Met Mag 106 p 154-164, Meteorological Office, HMSO

Munn, R E 1966 "Descriptive Micrometeorology" Academic Press, New York

Murray, R 1977 "The 1975/76 Drought over the United Kingdom - Hydrometeorological Aspects". Met Mag 106, p 129-145, Met Office, HMSO

Penman, H L 1949 "The dependence of transpiration on weather and soil conditions". J Soil Science 1 1949

Perry, A H 1976 "The long drought of 1975/76" WEATHER, 31, No 10 p 328-334

Priestley, C H B 1959 "Turbulent Transfer in the Lower Atmosphere" University of Chicago Press, p 19-38

Ratcliffe, R A S 1976 "The Hot Spell of Late June-Early July 1976" WEATHER, 31, No 10 p 355-357

Ratcliffe, R A S 1977 "A synoptic climatologist's viewpoint of the 1975/76 Drought", Met Mag. 106 p 145-54.

Shaw, M S	1977	"The Exceptional heat-wave of 23 June to 8 July 1976". Met Mag 106 p 329-346
Sutton, O G	1953	"Micrometeorology"p 238 McGraw Hill Book Co Inc

List of Figures

x- - - - x Net radiation, R_N

x———x Soil heat flux, G

•··········• Latent heat flux, λE

⊙———⊙ Sensible heat flux, H

+———+ Maximum temperature, T_{max}

FIG 4: Hourly Energy Budget (0600-1800 GMT) with Cloud cover and screen temperature

(a) 20 June 1976 (c) 30 June 1976

(b) 26 June 1976 (d) 16 August 1976

x- - - - - x Net radiation, R_N

x———x Soil heat flux, G

+———+ Screen Temperature, T

•··········• Latent heat flux, λE

⊙———⊙ Sensible heat flux, H

FIG 5: Daily Evaporation from water and from grass at Cardington during Hot Spell 1.

FIG 6: Calculation of Boundary Layer Heating on 3 days using Cardington BALTHUM soundings

FIG 7: Temperature structure of the surface layer during a clear day.

FIG 8: Variation of Soil Heat Flux with Depth at Cardington - 26 June 1976.

FIG 9: Diurnal variation of Soil Heat Flux at Cardington: 25-27 June 1976.

TABLE 1: Comparison of Observed and Theoretical Soil Heat Flux Amplitudes on 26 June 1976.

THE PRINCIPAL COMPONENTS OF THE ENERGY BALANCE OVER A HORIZONTAL SURFACE

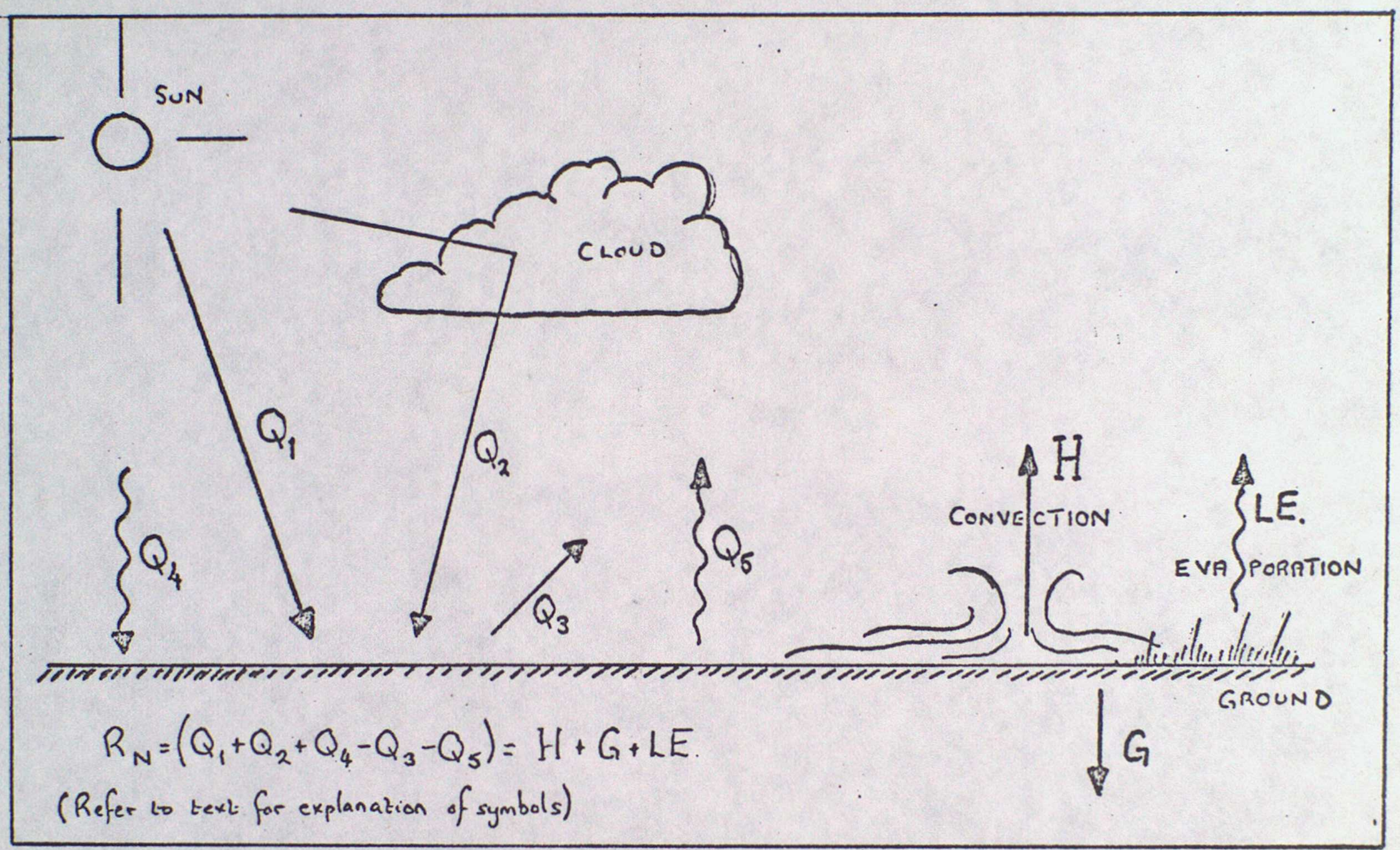

FIG. 1

MONTHLY EVAPORATION AND RAINFALL - CARDINGTON - MARCH TO OCT 1976

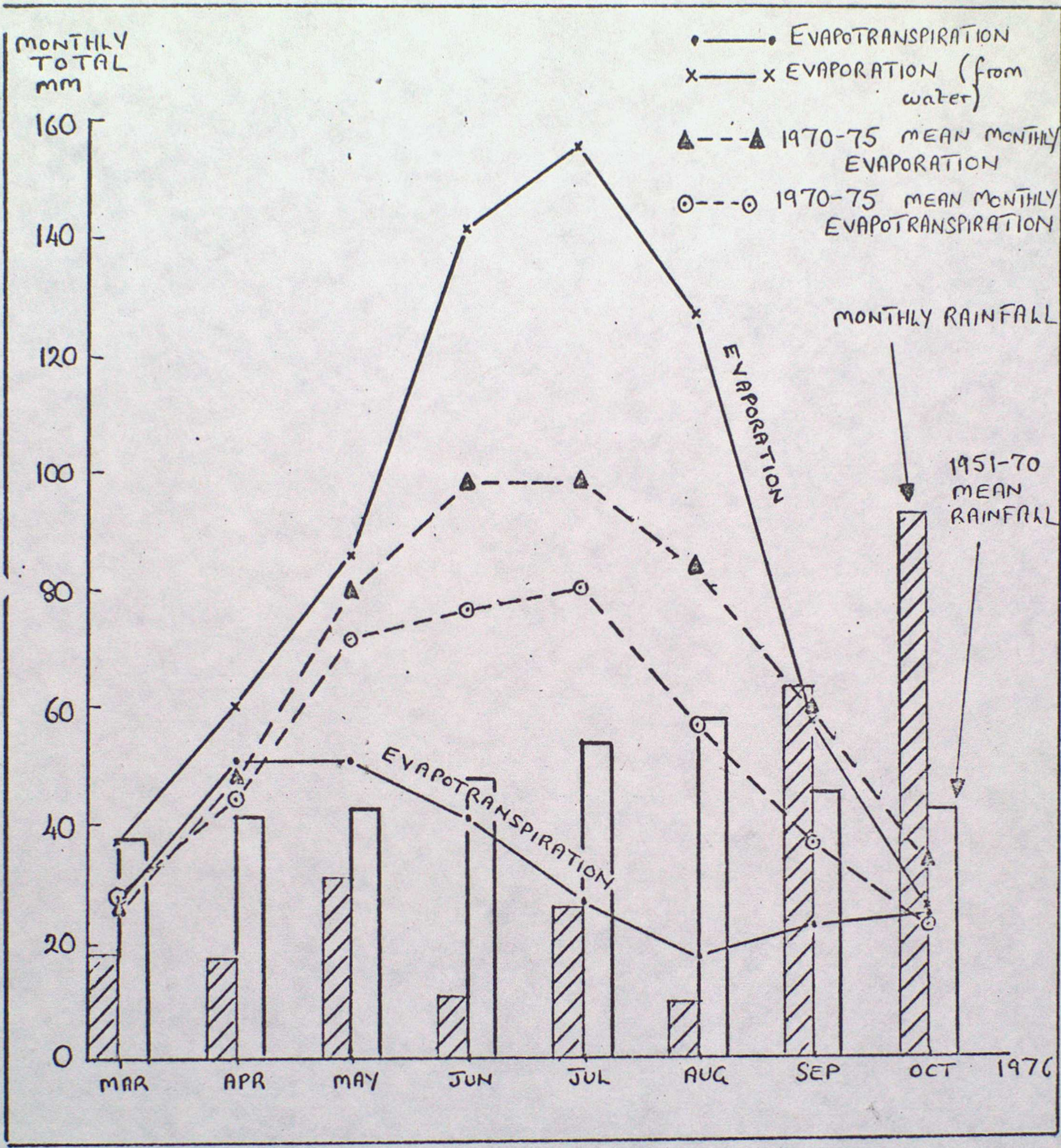

FIG. 2.

FIG. 3

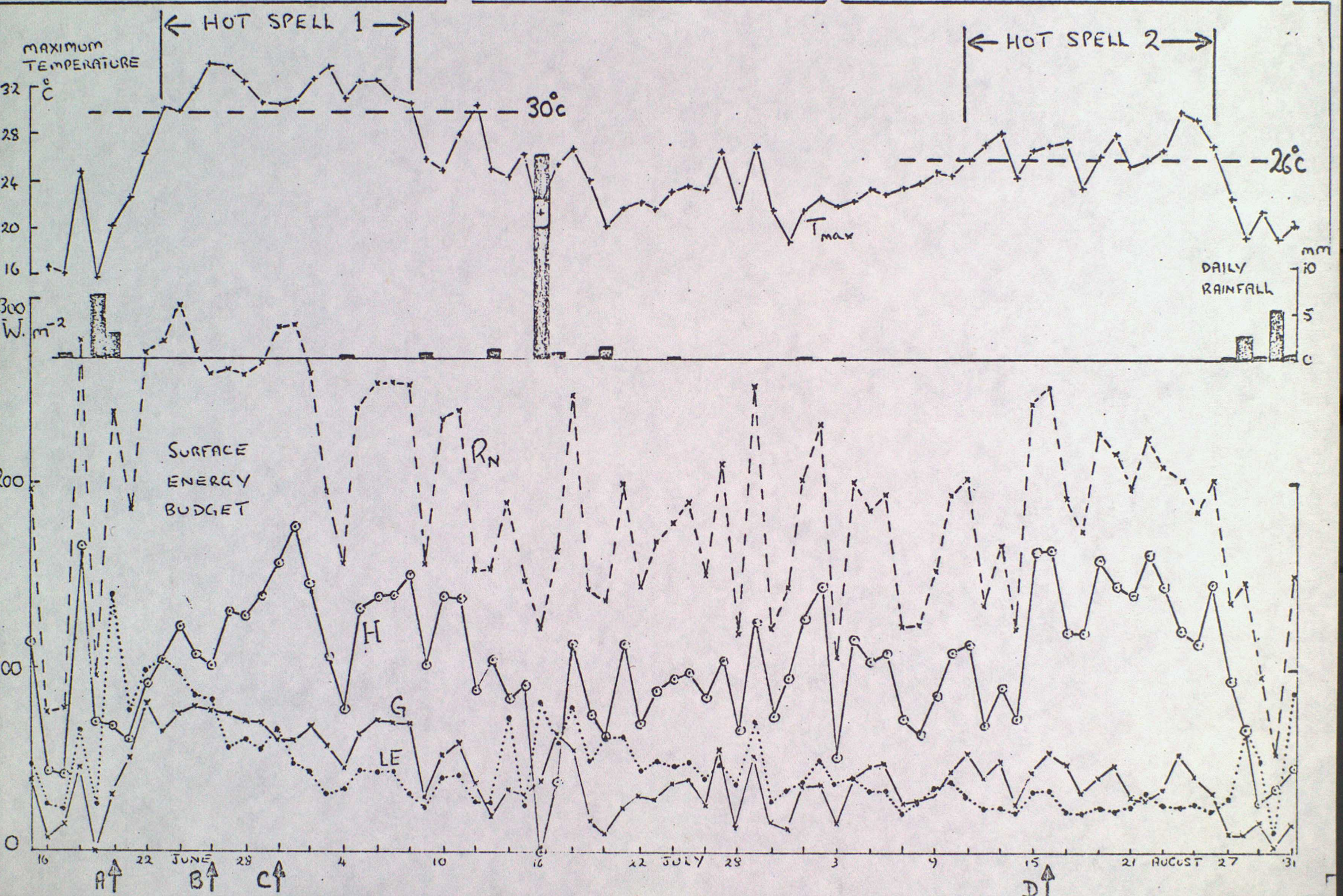

← HOT SPELL 1 →
← HOT SPELL 2 →
MAXIMUM TEMPERATURE
°C
32
28
24
20
16
30°C
26°C
T_{max}
DAILY RAINFALL
mm
10
5
0
300
W.m⁻²
200
00
0
SURFACE ENERGY BUDGET
R_N
H
G
LE
16
22
JUNE
28
4
10
16
22
JULY
28
3
9
15
21
AUGUST
27
31
A
B
C
D

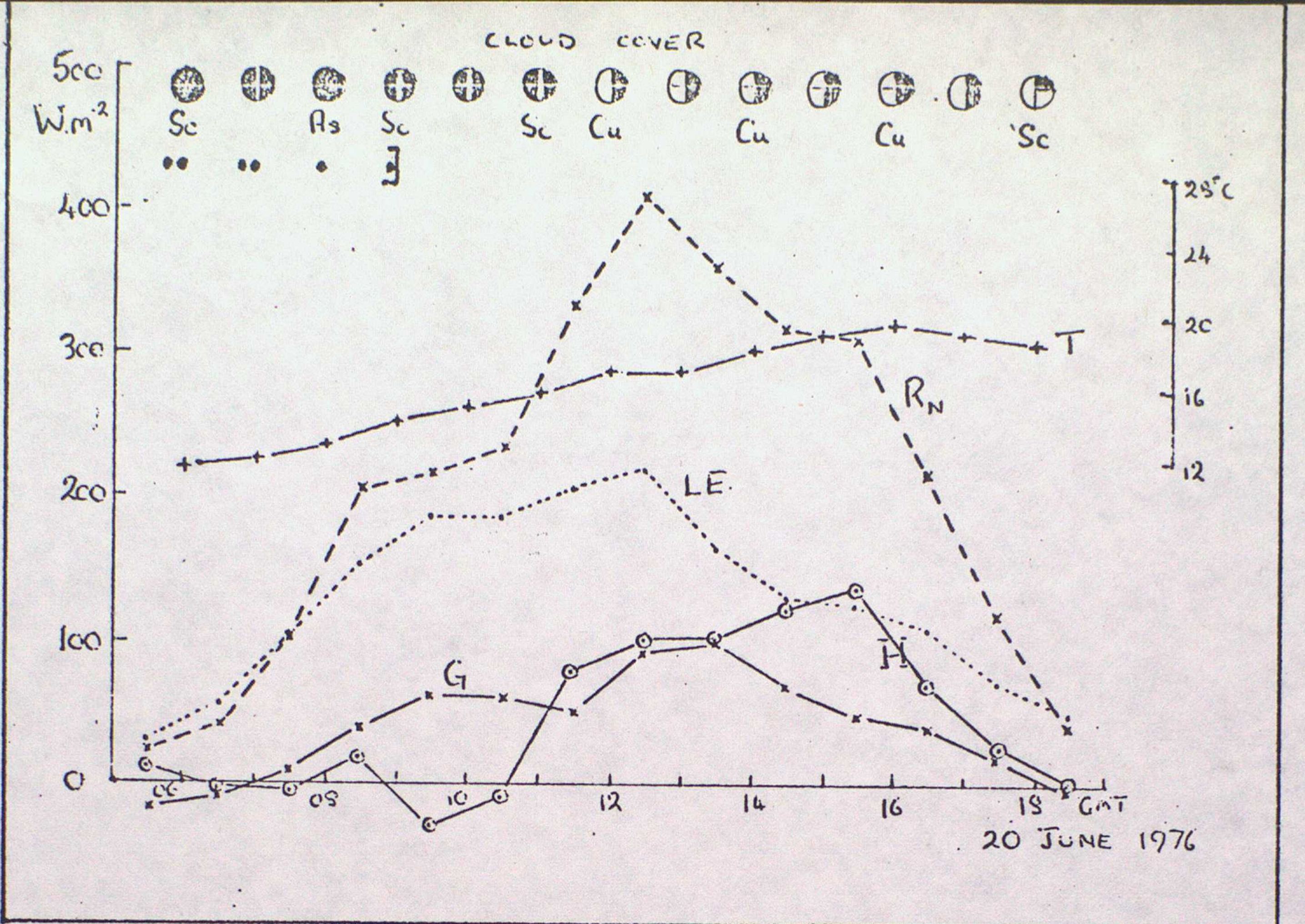

CLOUD COVER
500
W.m⁻²
Sc
As
Sc
Sc
Cu
Cu
Cu
Sc
400
300
200
100
0
25°C
24
20
16
12
T
R_N
LE
H
G
06
08
10
12
14
16
18
GMT
20 JUNE 1976

FIG. 4a

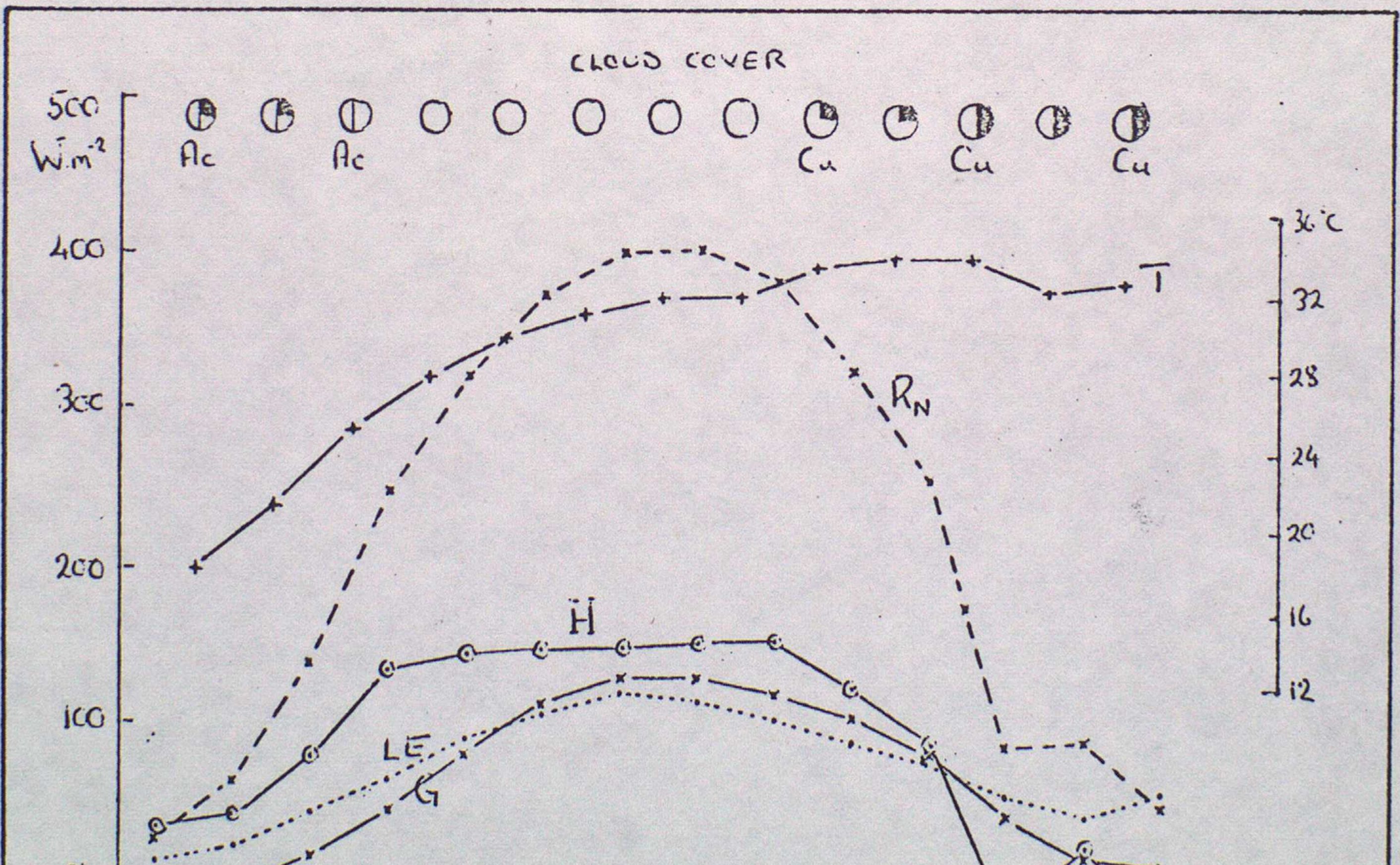

CLOUD COVER
500
W.m⁻²
Ac
Ac
Cu
Cu
Cu
400
300
200
100
0
36°C
32
28
24
20
16
12
T
R_N
H
LE
G
06
08
10
12
14
16
18
GMT
26 JUNE 1976

FIG. 4b

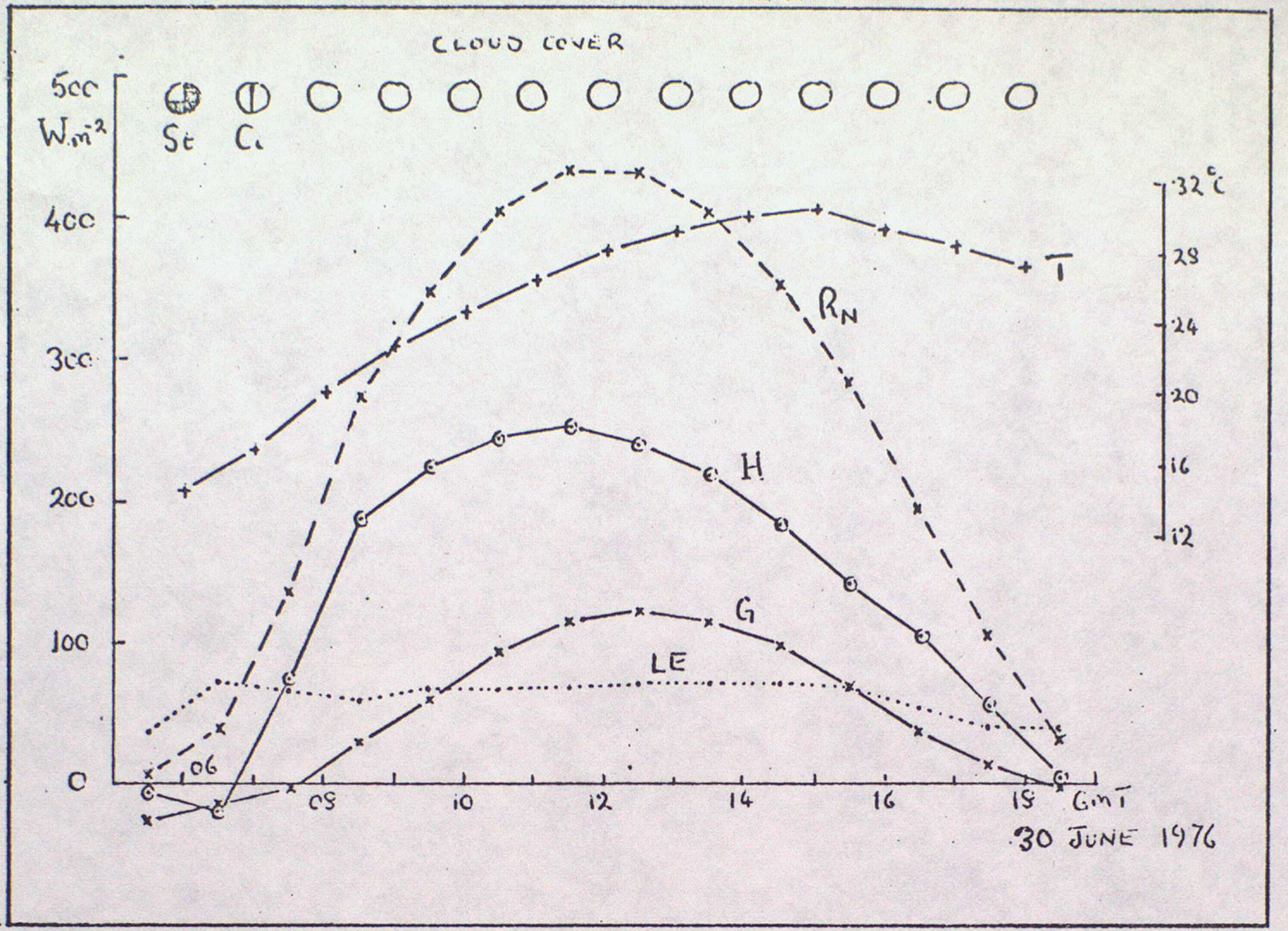

CLOUD COVER
500
$W\,m^{-2}$
St
Ci
400
300
200
100
0
06
08
10
12
14
16
18
GMT
30 JUNE 1976
32°C
28
24
20
16
12
T
R_N
H
G
LE

FIG. 4c

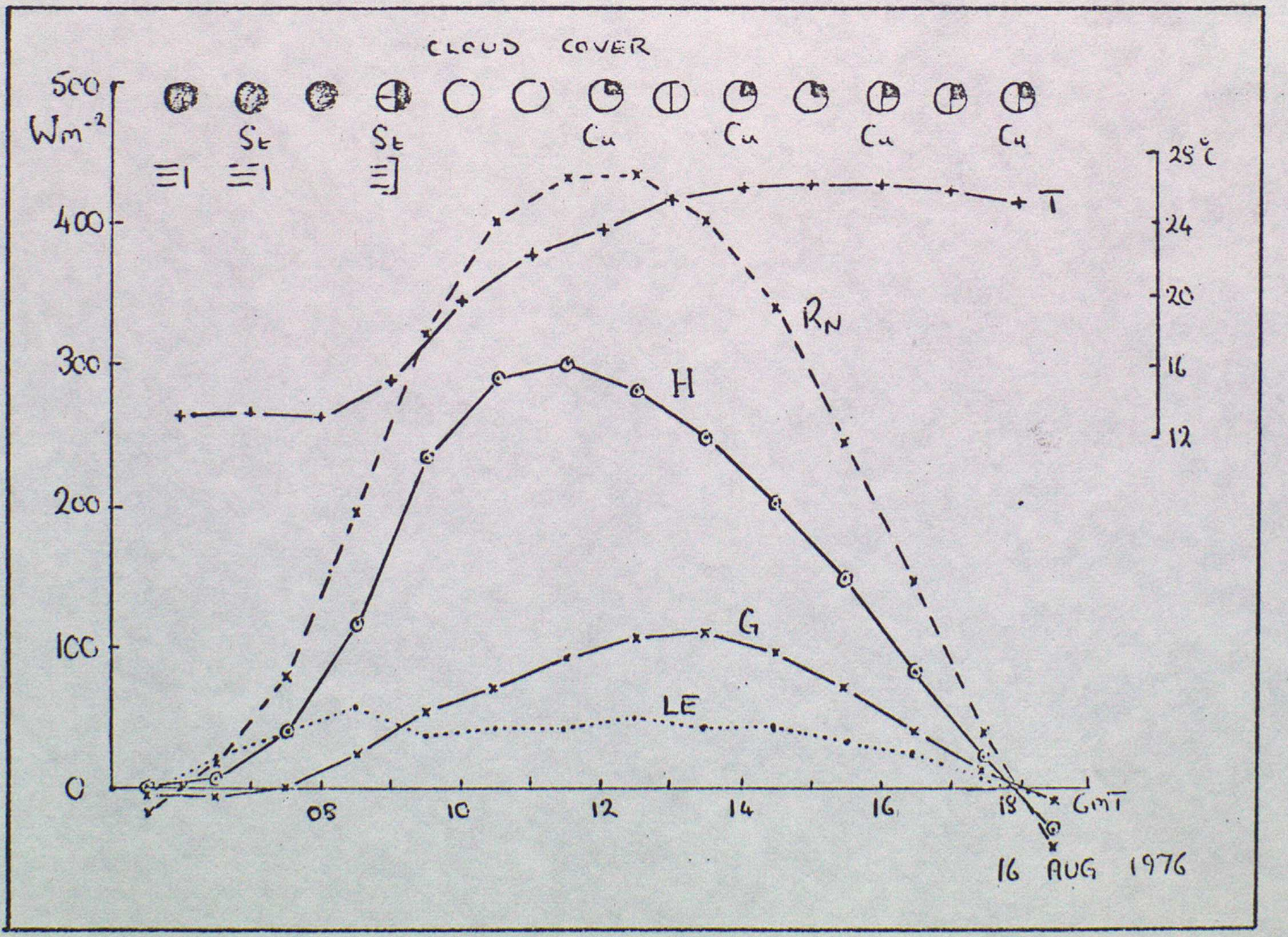

CLOUD COVER
500
$W\,m^{-2}$
St
St
Cu
Cu
Cu
Cu
400
300
200
100
0
08
10
12
14
16
18
GMT
16 AUG 1976
28°C
24
20
16
12
T
R_N
H
G
LE

FIG. 4d

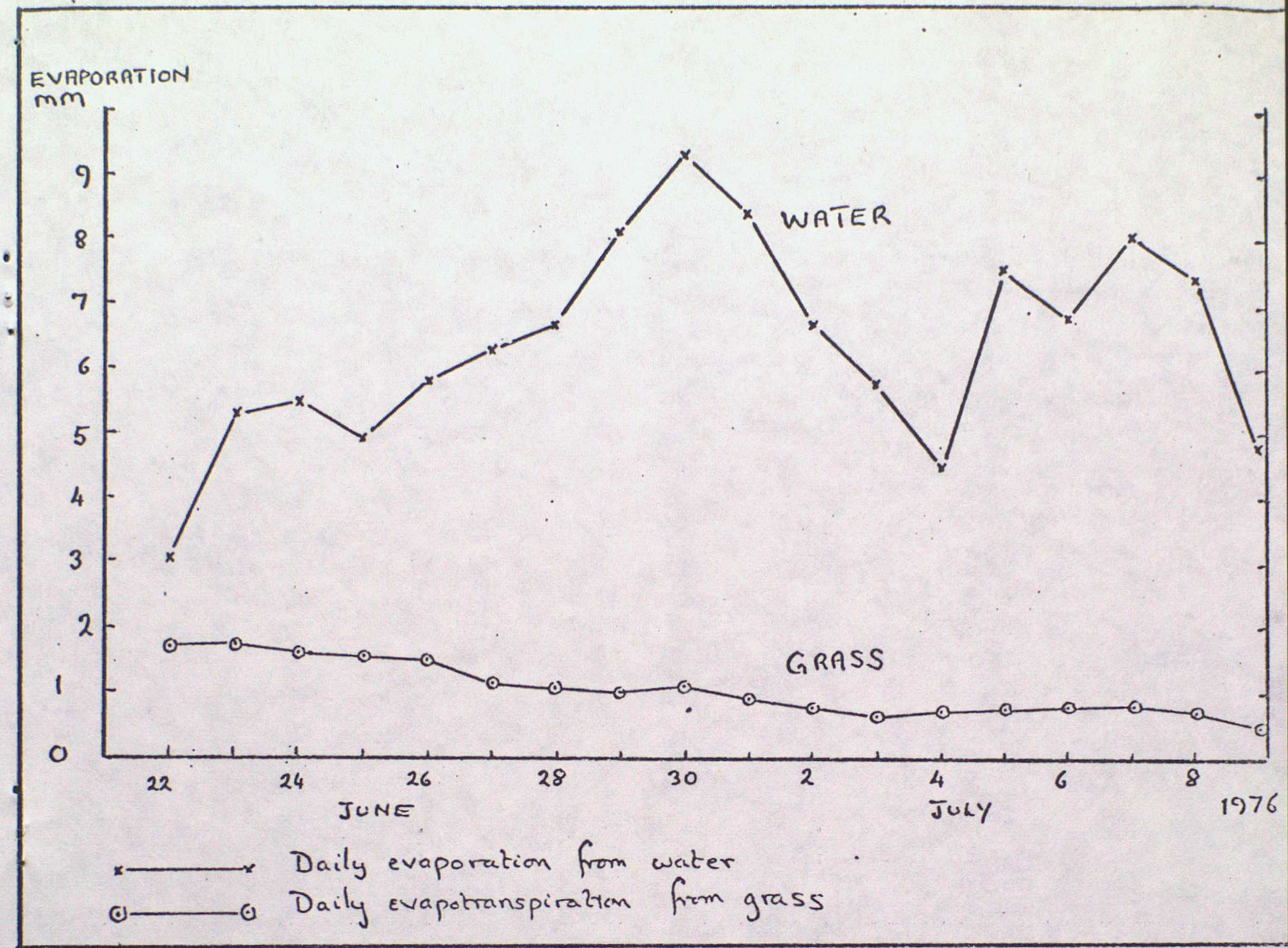
EVAPORATION
mm
0
1
2
3
4
5
6
7
8
9
WATER
GRASS
22
24
26
28
30
2
4
6
8
JUNE
JULY
1976
Daily evaporation from water
Daily evapotranspiration from grass

FIG. 5

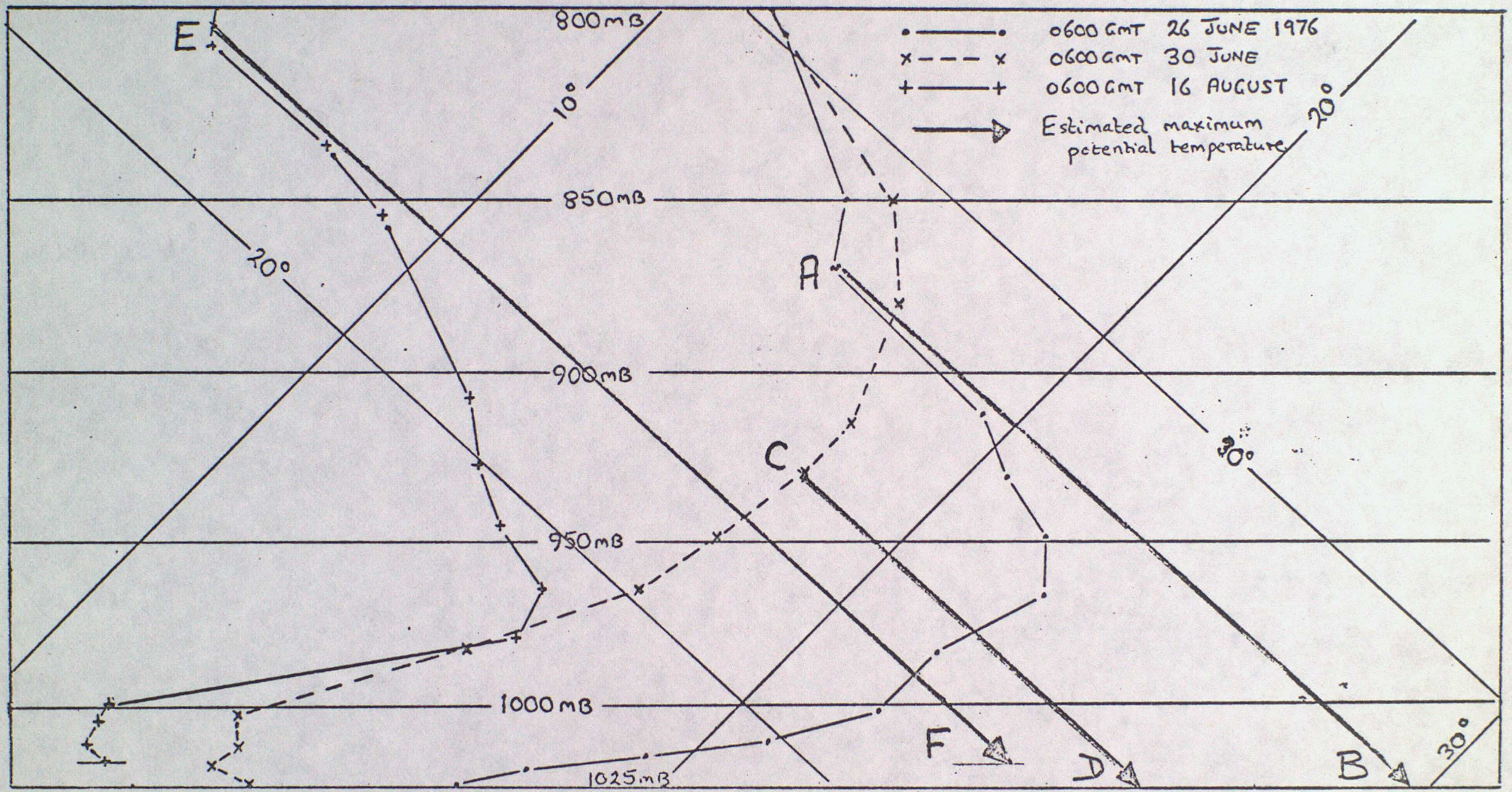
0600 GMT 26 JUNE 1976
0600 GMT 30 JUNE
0600 GMT 16 AUGUST
Estimated maximum potential temperature
800 mB
850 mB
900 mB
950 mB
1000 mB
1025 mB
10°
20°
20°
30°
30°
A
B
C
D
E
F

FIG. 6

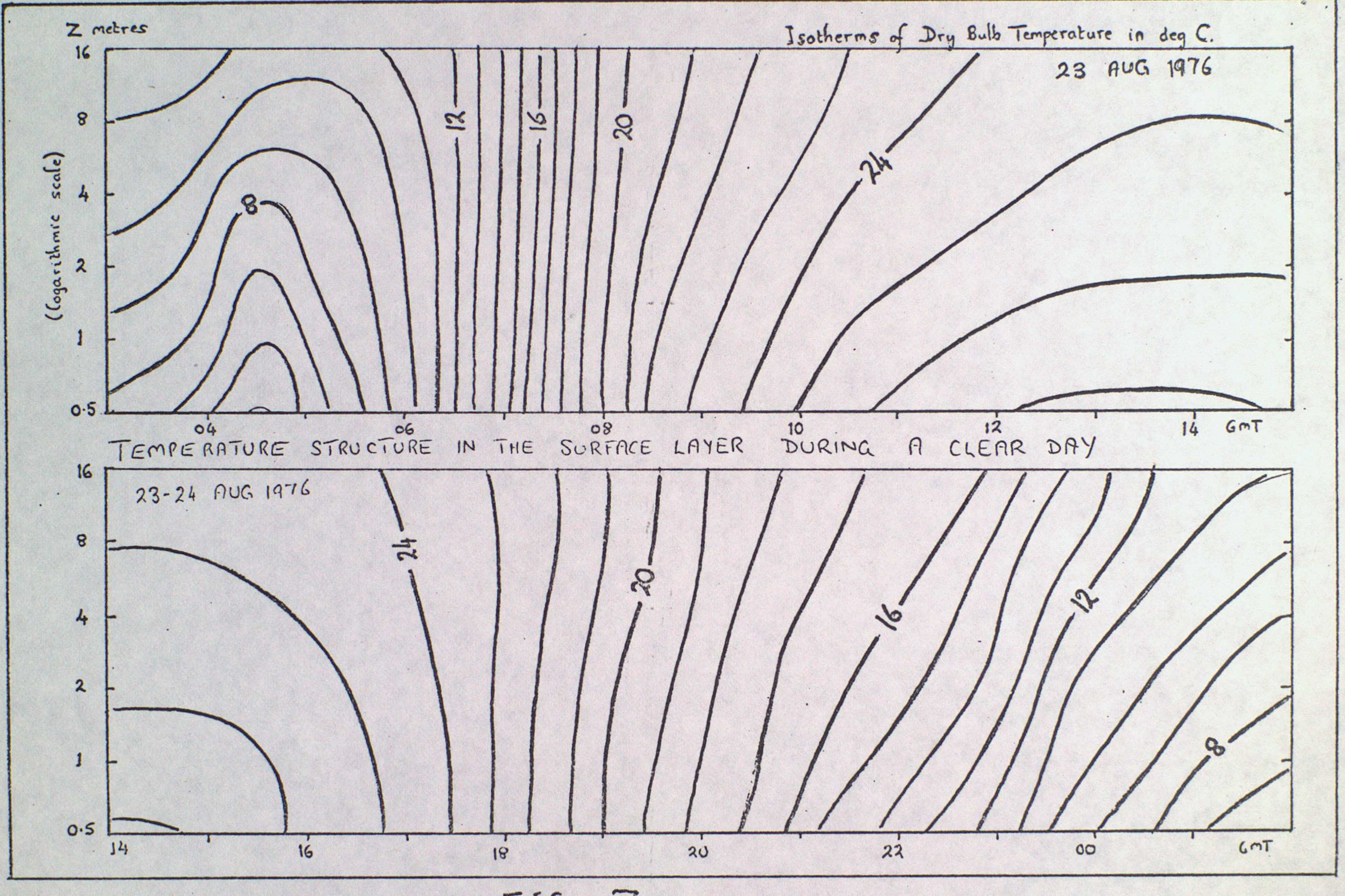
Z metres
Isotherms of Dry Bulb Temperature in deg C.
23 AUG 1976
(Logarithmic scale)
16
8
4
2
1
0·5
8
12
16
20
24
04
06
08
10
12
14
GMT
TEMPERATURE STRUCTURE IN THE SURFACE LAYER DURING A CLEAR DAY
23-24 AUG 1976
16
8
4
2
1
0·5
24
20
16
12
8
14
16
18
20
22
00
GMT

FIG: 7

VARIATION OF SOIL HEAT FLUX WITH DEPTH AT CARDINGTON — 26 JUNE 1976

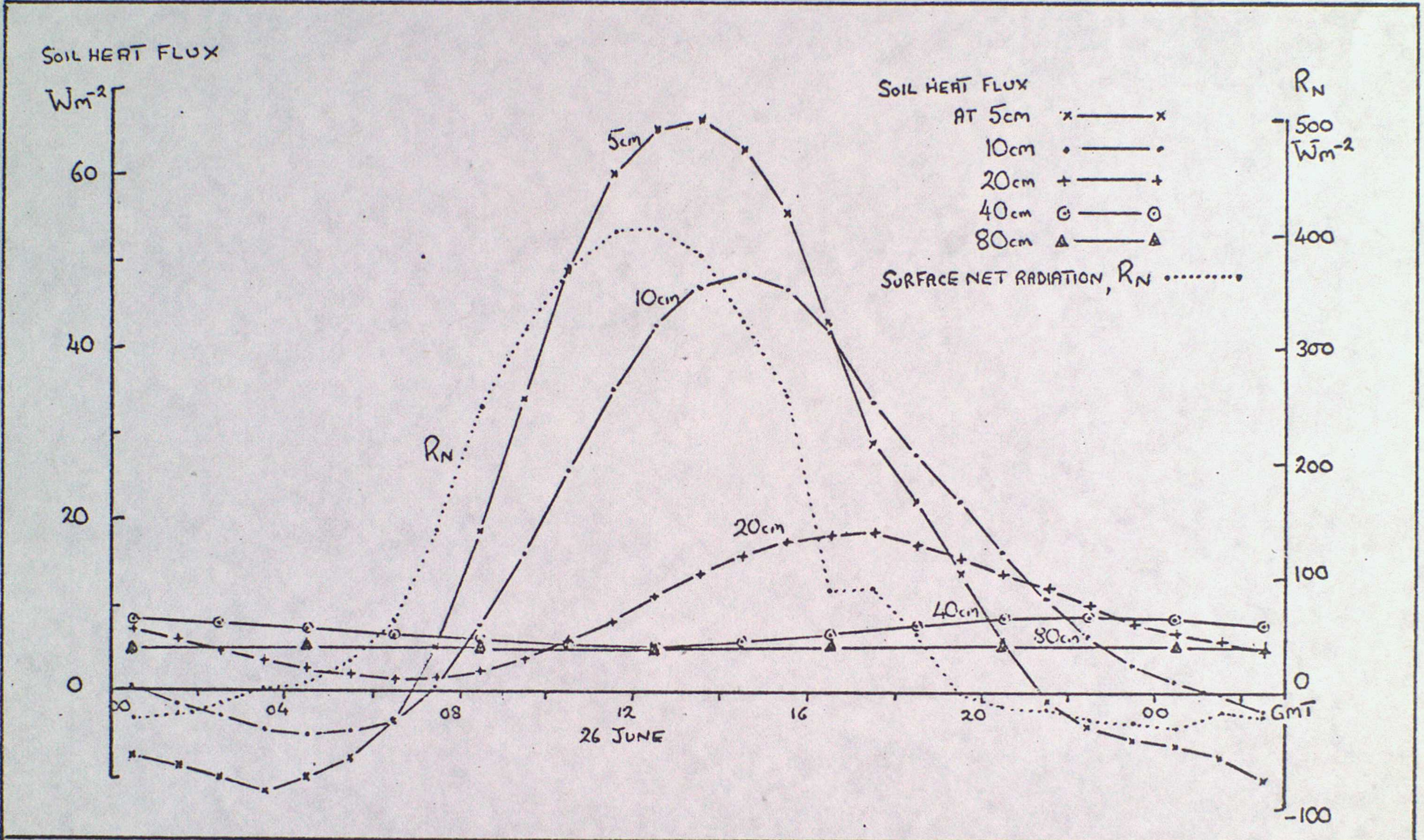

FIG. 8

DIURNAL VARIATION OF SOIL HEAT FLUX AT CARDINGTON : 25-27 JUNE 1976

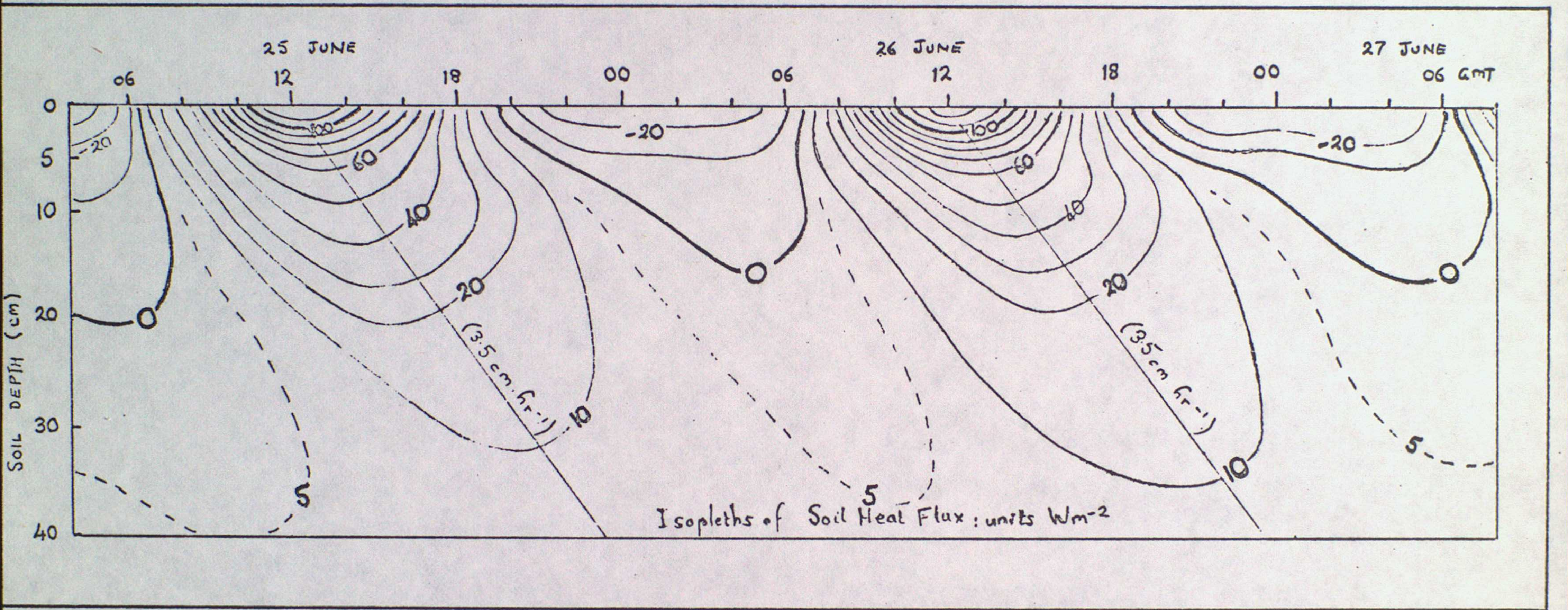

FIG. 9

1 DEPTH Z, cm	2 A_z/A_5 percent.	3 Actual Amplitude $W.m^{-2}$	4. Predicted Amplitude $W.m^{-2}$
0	156.8	120	105
5	100.0	67	67
10	63.8	43	43
20	26.0	12	17
40	4.3	2	3

TABLE. 1.